Fundamental Research 4 (2024) 1025–1035

Contents lists available at ScienceDirect

Fundamental Research

journal homepage: http://www.keaipublishing.com/en/journals/fundamental-research/

Article

Uncovering the CO_2 emissions of vehicles: A well-to-wheel approach

Zuoming Zhang[a,1], Hongyang Su[a,1], Wenbin Yao[b,1], Fujian Wang[c], Simon Hu[d], Sheng Jin[c,e,*]

[a] Polytechnic Institute & Institute of Intelligent Transportation Systems, Zhejiang University, Hangzhou 310058, China
[b] School of Civil Engineering and Architecture, Zhejiang Sci-Tech University, Hangzhou 310018, China
[c] Institute of Intelligent Transportation Systems, College of Civil Engineering and Architecture, Zhejiang University, Hangzhou 310058, China
[d] Zhejiang University/University of Illinois at Urbana-Champaign Institute (ZJU-UIUC Institute), Haining 314400, China
[e] Alibaba-Zhejiang University Joint Research Institute of Frontier Technologies, Hangzhou 310027, China

ARTICLE INFO

Article history:
Received 30 March 2023
Received in revised form 18 June 2023
Accepted 21 June 2023
Available online 16 July 2023

Keywords:
Carbon neutrality
Well-to-wheel emission
Emission characteristics
License plate recognition data
Geographical and temporal weighted regression model
Emission reduction policy

ABSTRACT

Carbon dioxide (CO_2) from road traffic is a non-negligible part of global greenhouse gas (GHG) emissions, and it is a challenge for the world today to accurately estimate road traffic CO_2 emissions and formulate effective emission reduction policies. Current emission inventories for vehicles have either low-resolution, or limited coverage, and they have not adequately focused on the CO_2 emission produced by new energy vehicles (NEV) considering fuel life cycle. To fill the research gap, this paper proposed a framework of a high-resolution well-to-wheel (WTW) CO_2 emission estimation for a full sample of vehicles and revealed the unique CO_2 emission characteristics of different categories of vehicles combined with vehicle behavior. Based on this, the spatiotemporal characteristics and influencing factors of CO_2 emissions were analyzed with the geographical and temporal weighted regression (GTWR) model. Finally, the CO_2 emissions of vehicles under different scenarios are simulated to support the formulation of emission reduction policies. The results show that the distribution of vehicle CO_2 emissions shows obvious heterogeneity in time, space, and vehicle category. By simply adjusting the existing NEV promotion policy, the emission reduction effect can be improved by 6.5%–13.5% under the same NEV penetration. If combined with changes in power generation structure, it can further release the emission reduction potential of NEVs, which can reduce the current CO_2 emissions by 78.1% in the optimal scenario.

1. Introduction

Climate change has significantly affected the sustainable development of human society and the economy. The greenhouse effect caused by increasing emissions of greenhouse gases such as CO_2 is the main reason for global temperature rise. Many countries or organizations have introduced specific measures with corresponding deadlines to achieve carbon neutrality goals [1]. For example, the European Union (EU) has set a carbon neutrality vision for 2050, aiming to reduce greenhouse gas emissions by at least 50% by 2030 [2]. Meanwhile, China has established targets to peak carbon emissions by 2030 and achieve carbon neutrality by 2060. The primary sources of CO_2 emissions come from power generation and heating, industry and construction, and transportation. The transportation sector accounted for 15% of global annual CO_2 emissions in 2019 [3]. Road transport is a significant contributor to fossil fuel consumption and CO_2 production. It is estimated that road transport emissions account for over 80% of the transportation sector [4]. China has experienced rapid urbanization in recent years, with an increasing number of vehicles. By 2022, China's motor vehicle ownership reached 417 million, including 13.1 million new energy vehicles, a year-on-year growth of 67.13% [5]. The demands for passenger and freight transport and energy consumption show a rigid upward trend. The emissions share of the transportation sector may continue to grow in the future. Therefore, accurately assessing the CO_2 emissions generated by motor vehicles operating on roads becomes an urgent requirement for achieving carbon neutrality in transportation.

Vehicle emission inventories are effective methods for quantitatively estimating mobile source emissions and serve as essential foundations for developing emission reduction policies. The methods used to establish emission inventories include top-down approaches based primarily on macroscopic statistical data and bottom-up approaches centered on actual individual travel data [6]. Compared to the former, bottom-up approaches offer higher resolution [7–9], which allows for a more accurate estimation of CO_2 emissions at a micro-scale, tracks individual vehicle emissions, and demonstrates clear advantages. However, the requirement for large amounts of granular data, such as individual vehicle travel distances and speeds, limits the applicability of bottom-up methods, making it challenging to cover the majority of vehicles in urban

* Corresponding author.
E-mail address: jinsheng@zju.edu.cn (S. Jin).
[1] These authors contributed equally to this work.

https://doi.org/10.1016/j.fmre.2023.06.009

areas. On the other hand, the market for new energy vehicles, including battery electric vehicles (BEVs) and plug-in hybrid electric vehicles (PHEVs), has grown rapidly in recent years, gradually replacing traditional fuel vehicles worldwide. Emission inventories that previously focused primarily on fuel vehicles can no longer support future traffic regulation and effective emission reduction policies for road emission sources in the transportation sector. Although the application of clean energy vehicles is considered an essential means to reduce CO_2 emissions in transportation sector [10,11], further research is necessary to the evaluation of the actual emission performance of new energy vehicles (NEVs) fleets in cities. Additionally, while some studies have examined external factors [12–14] that influence vehicle emissions in cities, such as building environments, travel demands, population, land use, and fleet composition, the current understanding of the spatiotemporal heterogeneity relationship between complex road network characteristics, traffic state information, and vehicle emissions remains unclear.

Based on the above background, this paper used the well-to-wheel (WTW) method to calculate the fine-grained fuel life cycle CO_2 emissions of all vehicles based on license plate recognition (LPR) data. Then, trajectory reconstruction, complex network, and information entropy methods were used to extract the grid-based spatiotemporal characteristics of traffic state information, road network structure, built environment, socioeconomic attributes, and transportation infrastructure. The geographical and temporal weighted regression (GTWR), geographically weighted regression (GWR), and ordinary least squares (OLS) models were used and compared to analyze the spatiotemporal influencing factors of CO_2 emissions. Taking into account the vehicle behaviors, all vehicles on the road network were categorized to support in-depth analysis of the CO_2 emission contribution of vehicle. Finally, based on the above analysis, the influences of different emission reduction scenarios on vehicle CO_2 emissions are simulated to provide support for the formulation of CO_2 emission reduction policies.

The main innovations of this paper are as follows. (1) Extract individual vehicle trip chain and trajectory from LPR data, and establish a fine-grained fuel life cycle CO_2 emission inventory that includes NEVs. (2) Combined with vehicle travel behavior, the spatiotemporal CO_2 emission characteristics of urban vehicles were analyzed from multiple perspectives, and the effects of various emission reduction policies were evaluated. (3) Abundant spatiotemporal influencing factors of CO_2 emissions were constructed by combining trajectory reconstruction, complex network, as well as information entropy methods, and the spatiotemporal heterogeneity of CO_2 emissions was analyzed with the GTWR model.

The remaining sections of this study are organized as follows. Section 2 reviews existing research. Section 3 introduces the data and methodologies used in this study. Section 4 presents results and discussions. Finally, Section 5 provides conclusions.

2. Literature review

This study aims to establish a CO_2 emissions inventory for all vehicles in urban areas, including new energy vehicles, analyze the CO_2 emission characteristics of urban vehicles from multiple dimensions, and explore the impact of external environmental factors on vehicle CO_2 emissions. The literature review is conducted from two aspects: (1) estimation of urban vehicle CO_2 emissions and (2) analysis of emission influencing factors.

2.1. Estimation of urban vehicle CO_2 emissions

Currently, research on urban vehicular CO_2 emission inventories involves quantifying the emission characteristics of vehicles within specific temporal and spatial contexts. There are two approaches to establish an emission inventory according to different data sources and calculation methods: top-down approach and bottom-up approach [6]. The top-down approach generally estimates the total traffic emissions in a study area using macro statistical yearbook data, such as automobile ownership and vehicle kilometers traveled (VKT). Emissions are then spatially distributed to individual units based on specific characteristics like population density, road density, and traffic volume. In the case of limited data access and macro-scale emission research, the top-down approach is an effective method for emission estimation. However, it overlooks the dynamic changes and heterogeneity of road traffic, introducing biases during emission allocation and resulting in poor accuracy when estimating spatiotemporal emission distribution [15–17], which fails to precisely depict the spatiotemporal distribution characteristics of urban vehicles.

The bottom-up approach employs detailed vehicle activity data, such as vehicle types, emission standards, and driving trajectories, to estimate emissions generated by individual vehicles and aggregate them to different spatiotemporal scales, thereby achieving emission estimations at the individual vehicle and link levels. Although the emission inventories established through the bottom-up approach exhibit high resolution and accuracy, obtaining large-scale detailed vehicle activity data is challenging. Consequently, research subjects are typically limited to specific vehicles like buses, heavy-duty trucks [18], taxis [19], and other vehicles equipped with global positioning system (GPS). The emission inventories and thus cover only a small portion of road vehicles. Some studies introduce multi-source data to expand vehicle samples. For example, Liu et al. [20] calculated taxi fleet emissions using GPS data and estimated emissions based on the proportion of taxi numbers to the total number of vehicles detected by the LPR system within each spatial grid. They utilized a Gaussian process model to estimate emissions in areas not covered by detection devices. Zhou et al. [21] followed a similar approach by combining floating vehicle data, detectors, and manual field surveys, and extrapolate all vehicle emissions from link traffic volume and floating car emission. Wen et al. [22] trained a random forest model to predict traffic volume and average speed within grids based on land-use characteristics, subsequently deriving city-level vehicle emissions. However, these methods assume that the composition of vehicle fleets on roads is homogeneous, neglecting differences in vehicle performance and still failing to trace individual emissions for the entire urban vehicle fleet [23].

Moreover, most current statistical scopes for vehicle emission inventories primarily focus on direct emissions from fuel combustion during the operation of internal combustion engine vehicles (Tank-to-wheel, TTW stage emissions). Emissions produced during fuel production, processing, storage, and transportation (Well-to-tank, WTT stage emissions) are often overlooked in transportation sector emission accounting due to their relatively small proportions. As the automobile industry turns towards new energy, a large fleet powered by electricity and hydrogen will not directly generate emissions during operation but transfer the emission burden upstream [24–27]. Therefore, the WTT CO_2 emissions produced during energy production, storage, and transportation have a significant environmental impact that cannot be ignored [28].

In the process of achieving peak carbon and carbon neutrality in the transportation sector, it is unreasonable to emphasize zero emissions during operation while neglecting WTT stage emissions. Existing research based on the WTW analysis method has already studied the CO_2 emission reduction benefits of NEVs and traditional internal combustion engine vehicles. Although fossil fuel still plays an important part in electricity generation, some research results indicate that BEVs generally have lower equivalent emissions than existing internal combustion engine vehicles [29]. Moreover, BEVs driven by a nuclear-dominated power structure exhibit emissions as low as 9.7 g CO_2 eq/km [30]. However, studies estimating the emissions from NEV fleets during actual operation in urban environments remain scarce.

2.2. Analysis of factors influencing urban vehicle emissions

In recent years, with the acceleration of urbanization, the number of vehicles has rapidly increased, leading to prominent vehicle emission

problems [31]. The relationship between urban vehicle emissions and their external influencing factors has attracted widespread attention. Many studies have analyzed this issue from the perspective of the built environment. For instance, it was found that there is a negative relationship between population density and urban traffic emissions [32,33]. Simultaneously, population density is associated with compact urban layouts, and pursuing a compact urban development model will help reduce CO_2 emissions. Generally, higher road density corresponds to more vehicle emissions due to increased travel demand in areas with denser roads [34]. From land use perspective, the distance to the nearest bus station, the distance to the city center, employment density, and land use mixedness significantly influence vehicle CO_2 emissions, with threshold effects present [35]. Although existing research has identified some key factors related to urban traffic emissions using the built environment's 5D indicator system (density, design, diversity, distance to transit stops, and destination accessibility), it remains unclear how complex network indicators of road networks and time-varying traffic conditions influence urban traffic emissions. To our knowledge, the topological structure of urban road networks and dynamic traffic state information has a significant impact on emissions. For example, it was revealed by the complex network theory that some stations on the path of diffusion had a considerable effect on the NO_2 diffusion distribution in urban area [36]. Furthermore, research shows that there is a certain correlation between dynamic traffic state information (such as traffic speed and traffic intensity) and traffic-related CO concentrations in grids [37].

GTWR [38,39], as an extension of GWR [40], fully considers changes in both spatial and temporal dimensions. This makes the model more powerful in explaining the relationship between urban vehicle emissions and their external influencing factors. Although current research has recognized the spatiotemporal variation characteristics of urban vehicular emissions, the indicators adopted in modeling their influencing factors are still static [41]. This study extracts more potential influencing variables based on existing built environment variables. By incorporating time-varying traffic state indicators into the independent variables, the spatiotemporal heterogeneity of urban traffic emissions can be better modeled than that of incorporating static variables only based on GTWR. Thus, the GTWR model with time-varying variables provides a more comprehensive result for policy-maker to better understand spatial and temporal influencing factors of vehicle emissions, enabling fine management of urban transportation emissions.

3. Materials and methods

3.1. Materials

3.1.1. LPR data

LPR data refers to the real-time recordings of passing vehicles detected by cameras deployed in the road network. A detailed introduction to LPR data can be found in Supplementary Materials 1. This study is based on LPR data from the urban area of Hangzhou from April 19th to May 19th, 2021, and the distribution of LPR detectors is shown in Fig. 1a. A total of 2052 LPR devices were installed in the research area, and an average of 13 million records of passing vehicles were collected every day. In order to improve data quality, we performed data cleaning for original LPR data, including deleting error detection records and duplicate detection records. A detailed data cleaning process can be found in Refs. [42,43].

3.1.2. Road network data

This study obtained the road network data of the research area from the OpenStreetMap (OSM), and then cleaned and preprocessed the road network data, such as deleting redundant nodes and edges, self-loops, and extracting roads of four levels (trunk, primary road, secondary road, and tertiary road). Next, a total of 2695 nodes and 7055 road sections were extracted from the road network data in the research area, see Fig. 1b, and the road network topology was established. The road network topology provides geographic information and spatial connectivity of each road section, which can support vehicle trajectory extraction and road emission intensity calculation.

3.1.3. Points of interest data

Points of interest (POI) data refers to locations in electronic maps that represent places of interest such as commerce, services, culture, and tourism. The POI data used in this study was collected through the API interface provided by Amap [44]. The spatial distribution of POIs is shown in Fig. 1c. The original data was reclassified into six categories, including residential type, enterprise type, life service type, shopping type, public service type, and entertainment type. For the introduction and reclassification method of POI data, refer to the [45], and the details of reclassification can be found in Supplementary Materials 1.

3.2. Extraction of vehicle travel activity information

LPR data contains spatiotemporal information about vehicles, which can be used to extract vehicle trajectories. However, due to the limited detection equipment coverage [20], a part of the vehicle trajectories extracted from the LPR data is incomplete. This study reconstructed the vehicle trajectories and extracted driving activity information to provide a data basis for estimation of urban vehicle emissions. The specific steps are shown below:

The first step is to extract the trip chain of the vehicle. The LPR data is mapped onto the road network topology to associate the detectors with the intersections. Then the license plate number and timestamp are sorted to obtain the trip chain of each vehicle, as shown in Eq. 1:

$$T_{RA}^{a} = \left\{ \left(P_1^a, T_1^a\right), \ldots, \left(P_i^a, T_i^a\right), \ldots, \left(P_{n_a}^a, T_{n_a}^a\right) \right\} \tag{1}$$

where $T_{RA}{}^{a}$ represents the trip chain of vehicle a, $P_i{}^{a}$ represents the position of the ith point in the trip chain, $T_i{}^{a}$ represents the detected time of the ith detected point in the trip chain and n_a is the total number of detected points of vehicle a.

After extracting the trip chains for a vehicle, the travel time [46] between every two chronological detected points is calculated. We use a travel time threshold method to identify the break points of a trip chain and derive every single trip of the individual vehicle [47].

Next, the adjacent matrix of intersections is established. If a vehicle passes two intersections that are not adjacent in space successively, the trajectory segment is considered incomplete and needs to be reconstructed. For the incomplete trajectory segment, the K-shortest-path algorithm is used to select a reasonable set of possible routes for the missing trajectory segment. Five decision indicators of trajectory distance, the number of vehicle turns, the number of intersections, travel time, and high-grade road length ratio are calculated for each candidate route. The Technique for Order Preference by Similarity to Ideal Solution (TOPSIS) algorithm is used to rank the routes in the set and complete the missing trajectory segment with the top-ranked route [48]. The detailed process of trajectory reconstruction is described in Supplementary Materials 2.

3.3. Vehicle category identification

Different categories of vehicles have various spatiotemporal travel behaviors, therefore, their contribution to road CO_2 emissions also varies greatly [49,50]. In order to accurately depict the CO_2 emissions of different categories of vehicles, this study divides the vehicles in the road network into different categories based on their historical travel behaviors. The methodology of vehicle categorizing based on LPR data originates from [42]. In this study, vehicle category indicates a classification method determined by different travel behavior characteristics, e.g., commuting vehicles for commuting purposes and light commercial vehicles for sporadic travel needs. In Section 3.4, vehicle type indicates a classification method determined by vehicle weight and engine

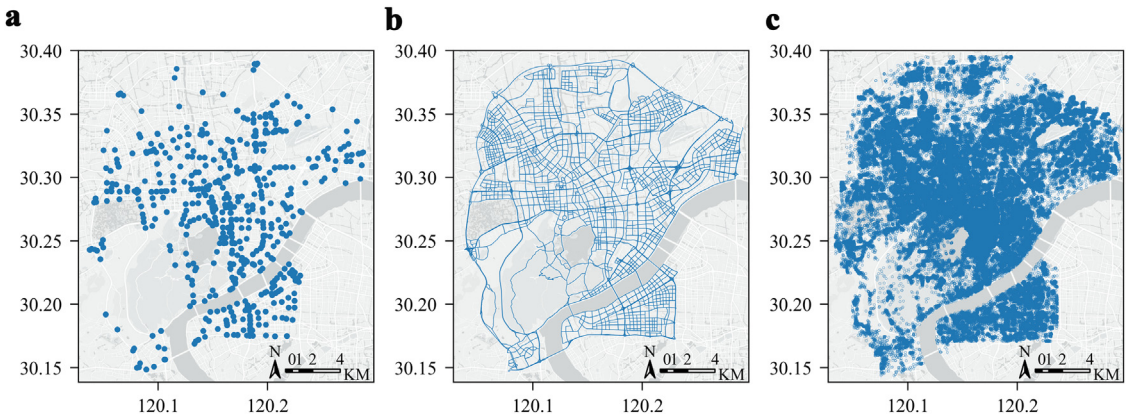

Fig. 1. Spatial distribution of the data. (a) Spatial distribution of the LPR detectors. (b) Road network in the research area. (c) Spatial distribution of POIs.

equipped, which is different from the vehicle category mentioned in this section.

The process of vehicle categorizing includes seven steps. First, filter out vehicles that have been detected very few times. To be exact, vehicles that are detected only one day are determined as vehicles that temporarily visit Hangzhou (TMPV), and vehicles that are detected once or twice daily are determined as vehicles passing through the research area (TRSV). Due to the low frequency of detection, there is little information contained in the LPR data of these two categories of vehicles, so their records were excluded in subsequent steps. Secondly, license plate number rules were used to directly identify heavy commercial vehicles (HCV), such as buses. Thirdly, based on LPR data, seven features reflecting the spatiotemporal travel behavior of vehicles were extracted. Fourthly, factor analysis was used to reduce the dimensions of the seven features to three linearly independent factors. The three factors are the regularity of travel behavior during peak hours, the regularity of travel behavior during off-peak hours, and the stability of origins and destinations during peak hours. In Step 5, the Iterative Self-Organizing Data Analysis Technique Algorithm (ISODATA) was used for clustering analysis, and the vehicles were divided into four clusters based on the three factors extracted in Step 4. Sixthly, based on the vehicle clustering result and the seven features extracted in Step 3, a decision tree model was trained to extract vehicle category identification rules for each category of vehicles. Finally, the vehicle category identification rule learned in Step 6 was used to quickly identify the vehicle categories of the entire fleet. After conducting vehicle categorizing based on the above framework, seven vehicle categories were successfully extracted, including light commercial vehicles (LCV), such as taxis, household spare vehicles (SPRV), daily household vehicles (DHV), commuting vehicles (CMTV), TMPV, TRSV, and HCV. See Supplementary Materials 3 for details.

3.4. Calculation of WTW emissions from vehicles

This study uses the WTW analysis method to develop a WTW emission factor model based on average speed to estimate CO_2 emissions of different vehicle types, coupled with vehicle travel activity information extracted from Section 3.2 to estimate emissions for different types of vehicles in the research area. Considering the sparseness of the trajectory data obtained from the LPR data. Before calculating vehicle emissions, make the following assumptions.

(1) Ignoring the sudden acceleration and deceleration of the vehicle, the vehicle travels at a uniform speed in each trajectory section.
(2) Considering only the hot emission of the vehicle.
(3) Ignoring the influence of weather conditions on CO_2 emissions.

According to the license plate color and coding rules, we identified six types of vehicles, including gasoline light duty vehicle (LDV), diesel heavy duty vehicle (HDV), light duty plug-in hybrid electric vehicle (LPHEV), heavy duty plug-in hybrid electric vehicle (HPHEV), light duty battery electric vehicle (LBEV) and heavy duty battery electric vehicle (HBEV). The WTW CO_2 emissions for a single vehicle trip are calculated by Eq. 2:

$$E_{i,j} = EF_{WTW,i} \times L_j \tag{2}$$

where i represents the vehicle types, j represents the road segment, $E_{i,j}$ is the CO_2 emission of vehicle type i on road segment j (g), $EF_{WTW,i}$ is the WTW equivalent CO_2 emission factor of vehicle type i (g/km), L_j is the length of road segment j (km). The specific calculation process of emission factors for models of six vehicle types is shown in Supplementary Materials 4.

The total emissions of vehicles E_{total} can be expressed as Eq. 3:

$$E_{total} = \sum_{i,j} E_{i,j} \tag{3}$$

where E_{total} represents the total emissions of vehicles in the study area.

3.5. Analysis of spatiotemporal factors affecting vehicle CO_2 emissions

3.5.1. Extraction of spatiotemporal influencing factors

Vehicle CO_2 emissions are related to various factors such as the traffic state of the road network, the road network structure, the built environment, the socioeconomic attributes, and the transport infrastructure. To explore the spatiotemporal influencing factors of vehicle CO_2 emissions, we extracted a total of 19 explanatory variables from the above five aspects. The symbol and description of each variable is shown in Table 1.

Multicollinearity analysis and spatial autocorrelation testing [51] were performed on independent variables, which is described in detail in Supplementary Materials 5, and the independent variables that failed the test were removed. Finally, x_1, x_4, x_7, x_{11}, x_{12}, x_{13}, x_{14}, x_{15}, x_{16}, x_{17}, x_{18}, x_{19} were included in the subsequent regression analysis model. The details of each variable can be found in Supplementary Materials 6.

3.5.2. Model building

Due to the significant spatiotemporal heterogeneity of vehicle CO_2 emissions, the GTWR model was used to model vehicle CO_2 emissions [52,53]. The structure of the GTWR model is shown in Eq. 4:

$$Y_i = \beta_0(u_i, v_i, t_i) + \sum_k \beta_k(u_i, v_i, t_i) X_{ik} + \varepsilon_i \tag{4}$$

where $\beta_k(u_i, v_i, t_i)$ is the regression coefficient at the ith spatiotemporal unit corresponding to the kth independent variable. In this study, the ith spatiotemporal unit refers to grid i at time t_i. The coefficient can be used to identify the heterogeneity of both temporal and spatial dimensions. $\beta_0(u_i, v_i, t_i)$ is the intercept term at each spatiotemporal unit. A

Table 1
Variables of spatiotemporal influencing factors.

Type	Variables	Description
Dependent variables	y	Hourly vehicle CO_2 emissions
Traffic state information	x_1	Hourly total vehicle flow
Road network structure characteristics	x_2	Average in-degree of intersections per grid
	x_3	Average out-degree of intersections per grid
	x_4	Average betweenness of intersections per grid
	x_5	Average importance of intersections per grid
	x_6	The density of streets per grid
	x_7	The number of intersections per grid
	x_8	Street circuity in each grid
	x_9	The density of edges in the network in each grid
	x_{10}	Orientation entropy per grid
Built environment characteristics	x_{11}	Proportion of residential type POI
	x_{12}	Proportion of enterprise type POI
	x_{13}	Proportion of life service type POI
	x_{14}	Proportion of commercial type POI
	x_{15}	Proportion of public service type POI
	x_{16}	Proportion of entertainment type POI
	x_{17}	Shannon entropy index reflecting land use diversity
Socioeconomic attributes	x_{18}	Population
Transport infrastructure characteristics	x_{19}	The distance to the nearest bus stop

detailed introduction to the GTWR model can be seen in Supplementary Materials 7.

The GTWR model can be used to analyze the spatiotemporal influencing factors of vehicle CO_2 emissions. In order to compare with the GTWR model, this study uses GWR and OLS models to analyze vehicle CO_2 emissions. The Akaike Information Criterion (AICc) and *R*-squared (R^2) are calculated to evaluate the performance of each model [54,55].

4. Results and discussion

4.1. Analysis of CO_2 emission characteristics

4.1.1. Spatial and temporal characteristics of emissions

The average full-day CO_2 emissions of weekdays and weekends are 4470 t and 4243 t, respectively, a difference of 4.4%. The 24-h CO_2 emission variations of weekday and weekend are shown in Fig. 2a. It is shown that weekday CO_2 emissions have morning and evening peaks, with the morning peak being more pronounced than evening peak, and the maximum hourly CO_2 emissions occur at 8:00 am, reaching 320 t. In contrast, the weekend curve does not have a clear peak of CO_2 emissions. However, in the early morning hours (0:00 am–3:00 am), weekend CO_2 emissions tend to be higher than that on weekday because there are more vehicle activities during the weekend wee hours. The morning CO_2 emission on weekend grows more slowly than that on weekday, reaching and maintaining a range of 250–300 t until the late afternoon, with CO_2 emission higher than that in the peak hours of weekdays.

In this paper, spatial CO_2 emissions were aggregated into 1 km × 1 km grids in the research area. The natural breaks classification method divides the CO_2 emission intensity of each grid into eight classes. According to Fig. 2b, **c**, the CO_2 emission hotspots in the area, colored in orange and red, are highly concentrated, with CO_2 emission intensity 4–8 times higher than that of the surrounding grids. The CO_2 emission hotspots are distributed along one east-west and two north-south corridors, corresponding to the distribution of the expressway in the research area. The north–south distribution of hotspots on the left corresponds to the Zhonghe elevated expressway and on the right to the Qiushi elevated expressway. In contrast, the grid of hotspots distributed east-west is the Desheng elevated expressway. The result indicates that vehicle activities on the expressway are the primary source of CO_2 emissions in study area.

Combining the spatial and temporal variation of vehicle CO_2 emissions, the chronological emission pattern can be observed at the city grid level, as shown in Fig. 2d, e. Generally, CO_2 emissions spread outward from the city center as vehicle activity increases**.** On weekday, the period with the least CO_2 emission is 3:00 am–6:00 am, followed by 0:00 am–3:00 am, while the CO_2 emissions of other periods are relatively consistent. The urbanization of the northwest corner of the research area is still in the initial stage, and the southwest corner is occupied by the mountains of the West Lake scenic area, both with low CO_2 emission intensity throughout the day. Fig. 2e shows that the spatial distribution of CO_2 emissions on weekend is similar to that of weekday. However, the CO_2 emission intensity on weekend is notably lower than that on weekday between 6:00 am and 9:00 am. In contrast, the CO_2 emission intensity during 0:00–3:00 on weekend is slightly higher than that on weekday during the same period, corresponding to the difference in the curve of the temporal distribution of CO_2 emissions.

4.1.2. Vehicle emission sharing rate

Table 2 shows the average emission factors and average daily travel intensities for different vehicle types. For vehicles with the same fuel type, the emission factor for heavy duty vehicles is 4–6 times that of light duty vehicles. In contrast, the emission factors for BEVs and PHEVs are 41%–53% and 57%–67% of that for fuel vehicles, respectively. The average travel intensity varies greatly among different vehicle types. NEVs are significantly higher than fuel vehicles, this may be attributed to the fact that NEV fleets include a large number of commercial vehicles such as online ride-hailing vehicles and buses.

Based on the CO_2 emission data of different vehicle types, the CO_2 emissions share of each vehicle type for 24 h are shown in Fig. 3a, b. The results show that LDVs are the first source of CO_2 emissions in all hours, accounting for 50% to 80% of the total CO_2 emissions. Although the number of HDV is only 4% of the total number of vehicles, they contribute more than 15% of the CO_2 emissions, especially in the late-night hours from 11:00 pm to 6:00 am. When heavy diesel vehicles such as garbage trucks, dump trucks, and cement mixers are concentrated in activities, the CO_2 emission share of HDV can reach more than 20%, highlighting the importance of controlling HDV CO_2 emissions for reducing the total vehicle CO_2 emissions. The CO_2 emission share of all NEVs, including BEVs and PHEVs, stands at 9.64%, slightly higher than their proportion of 9.24% in the vehicle fleet. Considering that NEVs in the fleet is predominantly used for commercial purposes, with a daily travel intensity 2–3 times that of fuel vehicles, the emission reduction contribution of using clean energy vehicles is still significant. Most of the CO_2 emissions from NEVs come from light vehicles, and the CO_2 emission contribution of heavy NEVs is mainly concentrated during the bus operating hours (5:00 am–9:00 pm).

Combined with the results of Section 3.3, we analyzed the average emission factors and average daily trip intensities of different vehicle

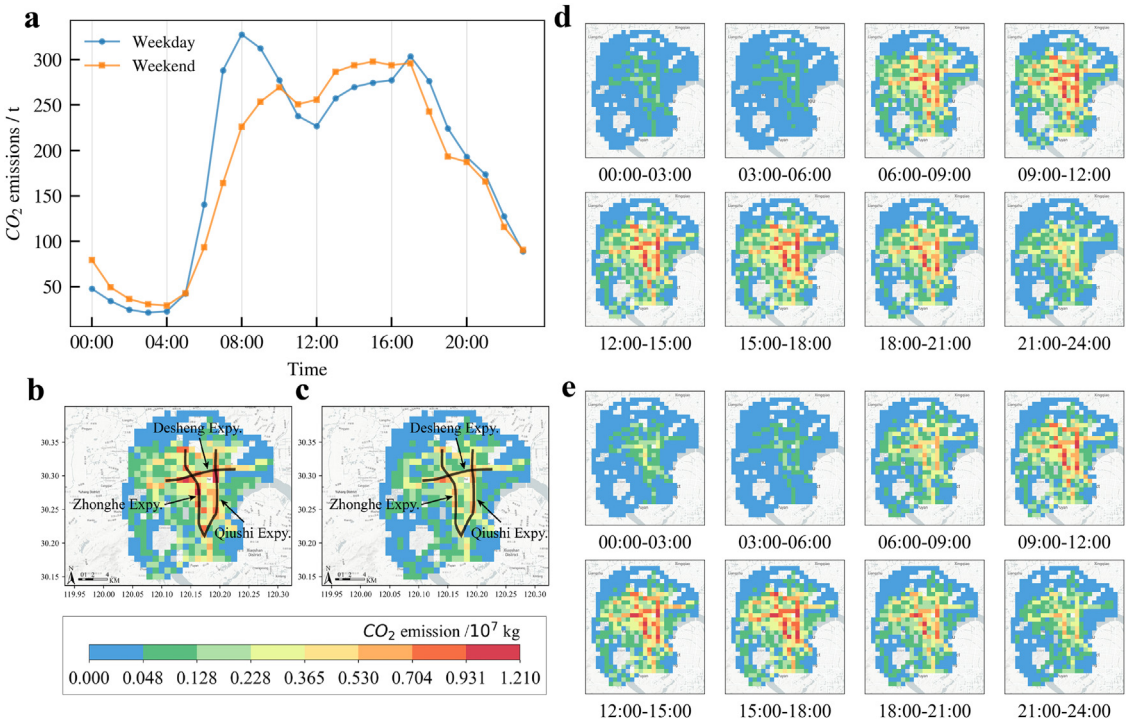

Fig. 2. Spatial and temporal distribution of CO_2 emissions in the research area. (a) 24-hour average CO_2 emissions of weekdays and weekends. (b) CO_2 emissions hotspots during weekday 6:00 am–9:00 am. (c) CO_2 emissions hotspots during weekend 6:00 am–9:00 am. (d) Distribution of diurnal CO_2 emissions on weekday. (e) Distribution of diurnal CO_2 emissions on weekend.

Table 2
Descriptive statistics for each type of vehicle.

Vehicle type	Average emission factor (g/km)	Average daily travel intensity (km/d)	Fleet share	Emission share
HDV	1089.8	19.2	4.0%	15.1%
LDV	249.8	18.9	86.8%	75.1%
HBEV	579.7	63.7	0.3%	2.1%
LBEV	101.5	34.5	5.9%	4.2%
HPHEV	617.8	49.1	0.1%	0.3%
LPHEV	167.9	33.4	3.0%	3.2%

Table 3
Descriptive statistics for each category of vehicle.

Vehicle category	Average emission factor (g/km)	Average daily travel intensity (km/d)	Fleet share	Emission share
SPRV	239.1	17.1	22.2%	16.6%
LCV	205.7	66.4	6.7%	17.3%
DHV	231.3	21.2	26.5%	24.0%
CMTV	239.8	15.1	23.6%	15.6%
TMPV	238.7	14.8	3.7%	2.4%
TRSV	238.9	11.6	13.1%	6.6%
HCV	965.1	22.4	4.3%	17.5%

categories, including LCV, SPRV, CMTV, DHV, TRSV, TMPV, HCV as summarized in Table 3. Except for HCV and LCV, the average emission factors of the other illustrated vehicles show slight variations. The three groups with the highest average daily trip intensity are LCV, HCV, and DHV.

Fig. 3c, d displays the emission shares of different vehicle categories at various periods. The results indicate specific differences in emission shares for different vehicle categories during different periods. SPRV, LCV, DHV, CMTV, and HCV are the primary sources of weekday emissions, while TRSV and TMPV contribute few, only accounting for 4%-13%. Among them, commercial vehicles, including light commercial vehicles such as online ride-hailing and taxi vehicles, and heavy commercial vehicles such as buses and trucks, have a significant proportion of the CO_2 emissions of off-peak hours at night. The CO_2 emission shares of CMTV significantly differ between peak and off-peak periods, reaching a maximum of 39% during the morning and evening peaks on weekday. In comparison, it is less than 10% during the remaining periods. In contrast, the CO_2 emission shares of SPRV and DHV are relatively stable, with slight variation over time. On the weekend, the CO_2 emission shares of all types of vehicles have changed, as shown in Fig. 3d. With the disappearance of morning and evening peaks, the sharing rate of CMTV no longer shows drastic fluctuations but remains stable at 10%–20% during the day. On the other hand, the CO_2 emission shares of

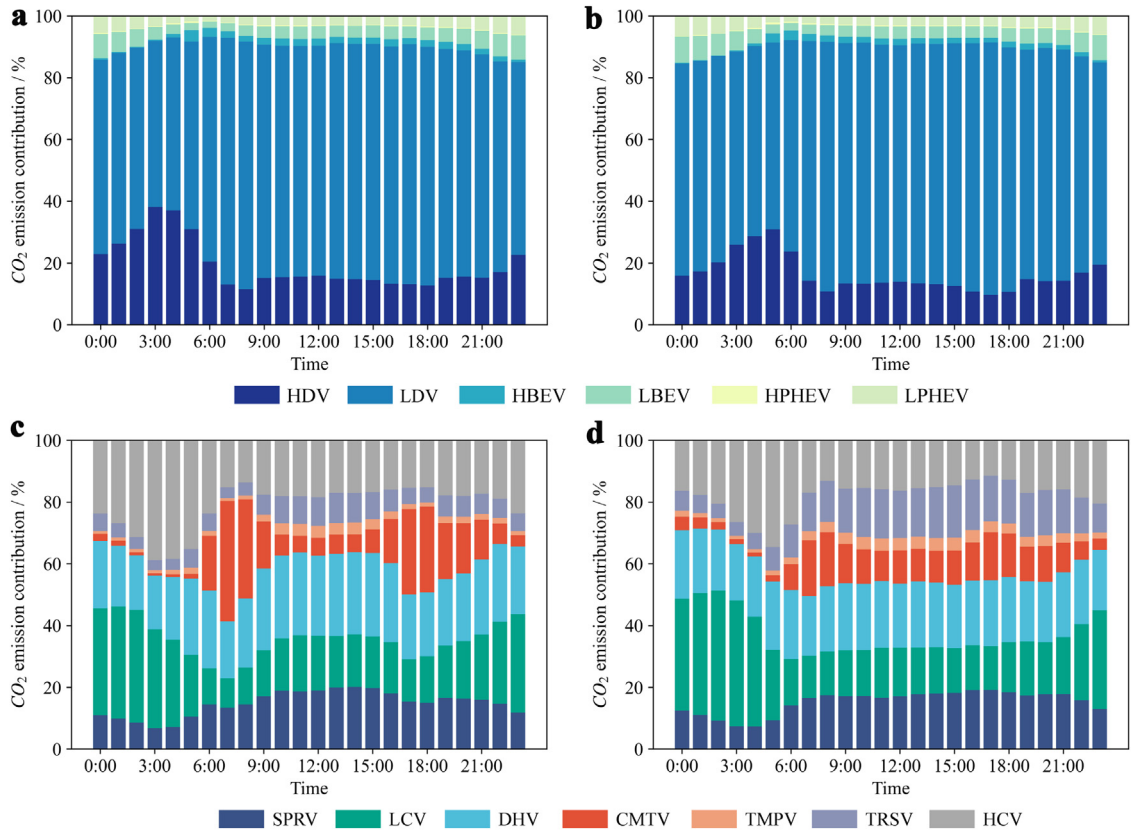

Fig. 3. Vehicle CO_2 emission share. (a) Different vehicle types on weekday. (b) Different vehicle types on weekend. (c) Different vehicle categories on weekday. (d) Different vehicle categories on weekend.

Table 4
Fitting effects of GTWR, GWR, OLS models.

Model	AICc	R^2
OLS	24460	0.591
GWR	18830	0.748
GTWR	1442	0.970

TRSV have significantly increased on weekend, which may be related to the increase in driving and sightseeing activities.

4.2. Analysis of vehicle CO_2 emission modeling results

Three models, GTWR, GWR, and OLS, were used to model vehicle CO_2 emissions, and the results obtained are shown in Table 4. It can be seen that the modeling effect of GTWR model on vehicle CO_2 emissions is significantly superior to GWR and OLS models.

(1) Temporal features of variable coefficients

Analyze the spatiotemporal influencing factors of vehicle CO_2 emissions from the temporal dimension, and take the average value of each variable according to the temporal dimension to obtain the coefficient changes at each hour, as illustrated in Fig. 4. Four independent variables, namely hourly total vehicle flow, average betweenness of intersections per grid, the number of intersections per grid, the distance to the nearest bus stop are shown to have a significant impact on vehicle CO_2 emissions, while the absolute values of the coefficients of the remaining variables at each hour are less than 0.1. The spatiotemporal characteristics of the coefficients of the remaining variables are illustrated in Figs. S2 and S3. The result indicates that traffic state information, road network structure characteristics, the built environment, socioeconomic attributes, and transport infrastructure characteristics all have significant impact on vehicle CO_2 emissions, with traffic state having the greatest impact on vehicle CO_2 emissions. Fig. 4a demonstrates a positive correlation between traffic volume and vehicle CO_2 emissions throughout the day, with the strongest correlation at morning peaks. There is also a positive correlation between the average betweenness of intersections and vehicle CO_2 emissions, and the correlation between the two is strongest at morning and evening peaks (Fig. 4b). The intersection betweenness can reflect the importance of the intersection to a certain extent. In the area with more important intersections, the more vehicle CO_2 emissions are, and this phenomenon is most obvious during morning and evening peak hours. Fig. 4c reveals a positive correlation between the number of intersections and vehicle CO_2 emissions, and this correlation is strongest at morning and evening peaks. The more intersections, the more vehicle CO_2 emissions will be. The Fig. 4d shows that there is a positive correlation between public transportation convenience and CO_2 emissions, which goes against our common sense on the surface. However, in combination with its spatial heterogeneity, we can further explore the reasons behind it.

(2) Spatial feature of variable coefficients

Analyze the spatiotemporal influencing factors of vehicle CO_2 emissions from the spatial dimension, and take the average value of each variable according to the spatial dimension to obtain the coefficient distribution of each grid, as shown in Fig. 5. The analysis of Fig. 5a reveals that traffic volume is positively correlated with vehicle CO_2 emissions in almost every grid, and the correlation is strongest in the center of Hangzhou, while the correlation is weaker in areas farther away from the center of the city. The traffic in the city center is already relatively congested, therefore, the increase in traffic volume has a significant effect on emissions. Furthermore, Fig. 5b, shows that the average betweenness of intersections exhibits significant spatial hetero-

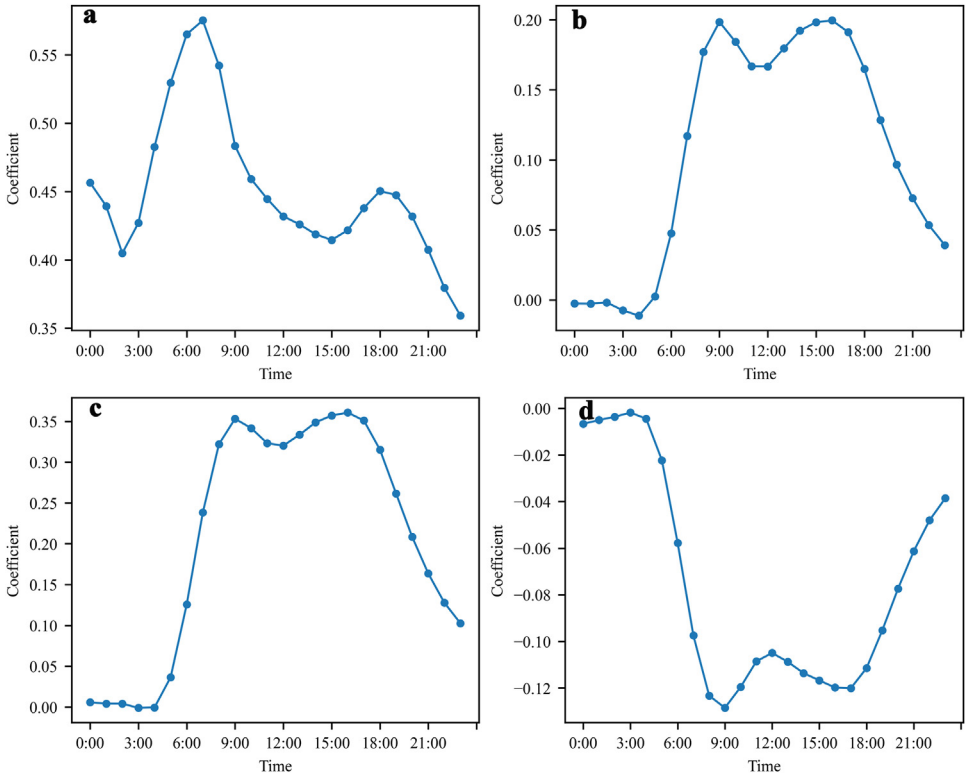

Fig. 4. Hourly average coefficient. (a) Hourly total vehicle flow variable. (b) Average betweenness of intersections per grid variable. (**c**) The number of intersections per grid variable. (d) The distance to the nearest bus stop variable.

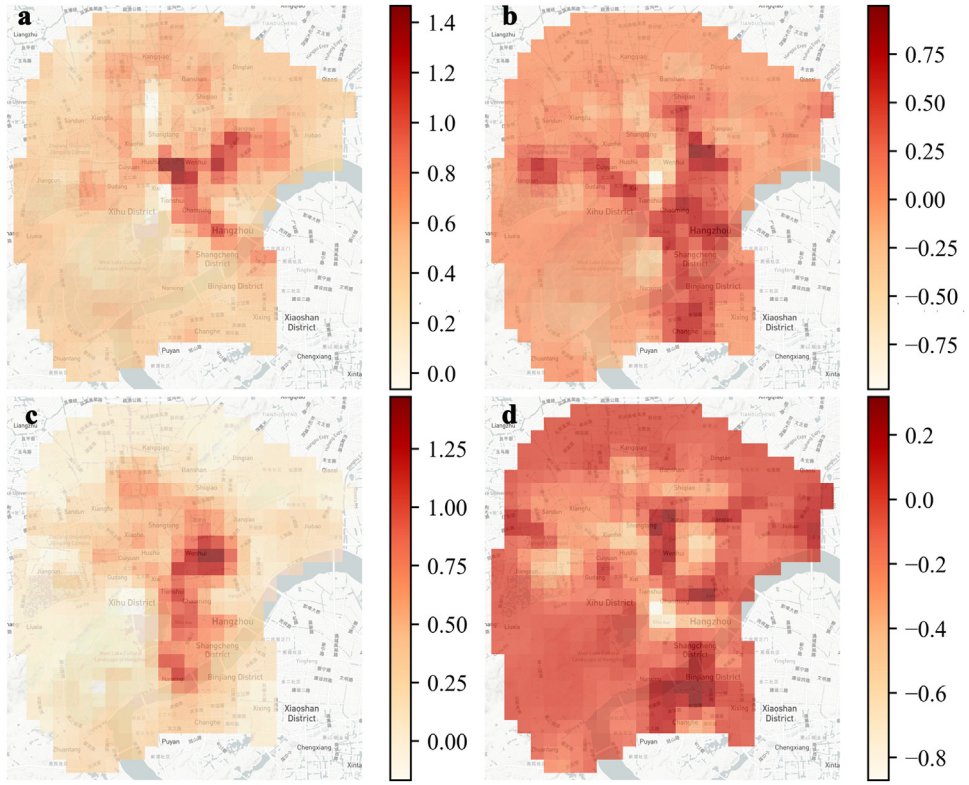

Fig. 5. Average coefficients of each grid. (a) Hourly total vehicle flow variable. (b) Average betweenness of intersections per grid variable. (c) The number of intersections per grid variable. (d) The distance to the nearest bus stop variable.

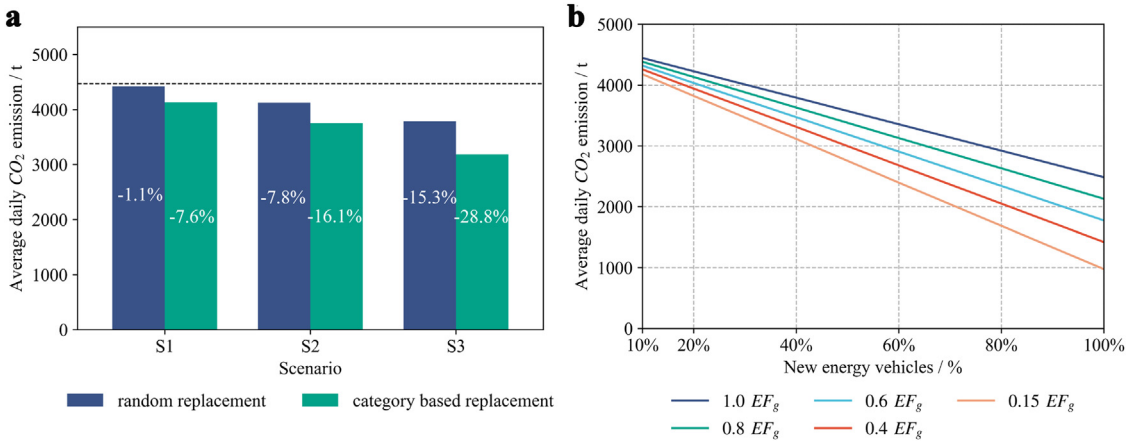

Fig. 6. The evaluation of simulated CO_2 emission reduction of different policies. (a) The comparison of CO_2 emission reduction under random replacement and vehicle category-based NEV promotion policies. The black dotted line represents the current average daily CO_2 emissions. (b) The synergistic CO_2 emission reduction effect of the NEV promotion and grid emission factor change.

geneity, with some areas showing a positive correlation, while others show a negative correlation. In some central areas of Hangzhou, there is a negative correlation between the two, which may be because the more important the intersections are in the central area of Hangzhou, the lower the proportion of vehicle trips due to parking and other issues. Fig. 5c indicates a positive correlation between the number of intersections and vehicle CO_2 emissions in most areas. This is because the more intersections there are, the greater number of stops during vehicle driving, leading to increased emissions. According to Fig. 5d, it can be seen that the convenience of public transportation facilities in most areas is negatively correlated with CO_2 emissions, while in few areas, the convenience of public transportation facilities is positively correlated with CO_2 emissions. The positive correlation in these areas is strong, resulting in a positive correlation in the overall time dimension.

4.3. Analysis of CO_2 emission reduction policies

(1) The impact of NEV promotion policies on urban vehicle CO_2 emissions

The transition from traditional fossil fuels to clean energy is crucial for achieving carbon peak and carbon neutrality in the transport sector. European countries have already announced their plans to ban the sale of fuel cars, while research conducted in China suggests that conventional fuel cars will be phased out completely by 2050 [56]. Government departments play an important role in promoting NEVs by reducing taxation, providing subsidies, constructing charging facilities, and other measures to encourage consumers to purchase NEVs. However, current NEV promotion policies do not consider the diverse travel patterns among different vehicle categories. For instance, LCVs, CMTVs, and DHVs have higher travel intensity and could achieve more emission benefits from switching to NEVs than other vehicles. Moreover, given that the operating cost per kilometer of a NEV is lower, those owners are more willing to replace their vehicles with NEVs [57]. This paper proposes that the government adopt incentive NEV promotion policies to prioritize the electrification of specific vehicle categories considering travel behavior, including LCV, DHV, and CMTV, for emission reduction. Three scenarios are explored to determine the emission reduction effects under different levels of NEV penetration, as shown in Table 5.

As a comparison, we randomly replaced the same proportion of traditional fuel vehicles from the entire fleet with NEVs according to the corresponding NEV penetration rate in each scenario, simulating the existing promotion policy without incline, and the emission reduction results under the two promotion policies are shown in Fig. 6a.

Table 5
Vehicle category based NEV promotion scenarios.

Scenario	Category of replacement	Number of replacement	NEV penetration
S1	LCV	40,413	11.2%
S2	LCV+CMTV	286,102	23.4%
S3	LCV+CMTV+DHV	562,114	38.8%

It is evident that the NEV promotion policy based on the vehicle category has great potential for emission reduction. In scenario S1, replacing fuel vehicles with NEVs in the LCV category can reduce daily CO_2 emissions by 7.6%, whereas randomly replacing the same number of vehicles can only reduce emissions by 1.1%. In scenarios S2 and S3, the incentive promotion policy can increase the emission reduction effect by 8.3% and 13.5%, respectively, compared with the random replacement strategy. Furthermore, under the 38.8% penetration of NEV, the incentive promotion policy can reduce the total CO_2 emission by up to 28.8%.

(2) The impact of grid CO2 emission factors on urban vehicle emissions

Currently, fossil fuel still dominates China's power generation structure. Especially in eastern China where Hangzhou is located, hydroelectric resources for power generation are generally lacking, and land resources required for photovoltaic and wind power generation are also relatively scarce. As a result, thermal power accounts for a relatively high proportion. In contrast, only 37% of the EU's electricity comes from fossil fuels [58]. With the promotion of NEVs leading to further expansion of electricity consumption, the upstream power generation still has a significant potential for emission reduction in the composition of future vehicle WTW emissions.

By adjusting the vehicle fuel type and grid emission factor, this paper numerically simulates the synergistic emission reduction effect of the increasing penetration of NEVs and the decreasing grid emission factor under the future deep emission reduction scenario. The current NEV penetration in Hangzhou is about 10%, and it is assumed that the penetration of NEV will gradually increase to reach 100% in the deep emission reduction scenario in future, while the proportion of power generated by fossil energy in China is expected to gradually decrease from the current 68% to 10% due to the substantial development of wind, nuclear power, and solar photovoltaic technologies [59,60]. Assuming that the CO_2 emissions from non-fossil energy generation are negligible and the structure of fossil energy generation remains unchanged, then the grid emission factor (EF_g) can be reduced to 0.15 times the current one (0.15 EF_g). Fig. 6b presents the changes in vehicle CO_2 emissions in

the research area under the comprehensive action of different grid CO_2 emission factor and NEV penetration during the process towards CO_2 neutrality.

The results demonstrate that the total CO_2 emissions decrease linearly with the increase in proportion of NEV in the fleet. In the early stage of electrification, when the NEV penetration is less than 20%, the change of the grid emission factor has little impact on the total CO_2 emission. Every 10% reduction of the grid emission factor can only reduce the CO_2 emission by about 30 t, accounting for 0.7%–1.1% of total emission. However, with the increase of NEVs, the emission reduction effect of reducing power grid emission factors becomes more significant. Finally, every 10% reduction in emission factors corresponds to a 4% reduction (355 t) in CO_2 emissions, which is more than ten-fold of the initial stage of vehicle fleet electrification.

Under the optimal emission reduction scenario, where the penetration rate of NEVs reaches 100% and the grid emission factor is reduced to 0.15 times the current one, the total CO_2 emissions can be reduced by 78.1% to 975 t. These findings highlight the potential of NEVs and renewable energy in contributing to China's emission reduction targets and suggest the importance of considering the joint effects of multiple emission reduction measures in the transport sector.

5. Conclusion

This paper proposes a framework for calculating the spatiotemporal CO_2 emissions of vehicles throughout the fuel life cycle, quantitatively analyzing the fine-grained emissions inventory of various categories of vehicles. And GTWR model is used to explore the spatiotemporal influencing factors of CO_2 emissions based on LPR data, road network data, and POI data. On this basis, the effects of different emission reduction policies are simulated.

The established emission inventory shows that the main emission hotspots are concentrated on the expressways in the city center, and the emission intensity can reach four to eight times that of the rest of the surrounding areas. Although the travel intensity of NEVs is greater than that of fuel vehicles, their emission factor is significantly lower than that of fuel vehicles. The highest proportion of CO_2 emissions is for LDVs, followed by HDVs. Regardless of the vehicle fuel type, the emission factors of heavy duty vehicles are significantly higher than those of light duty vehicles, with heavy duty vehicles accounting for 4.4% of the total number of vehicles contributing 17.5% of the emissions. Our results reveal great potential of CO_2 emission reduction through application of NEVs and emission control of heavy duty vehicles. Some actions may be practical for CO_2 emission reduction, such as mandatory replacement from traditional fuel vehicles to NEV for commercial vehicles, and planning low emission zone in the city center. Also, some insights for policymakers are not negligible. If the government adopts incentive NEV promotion policies, combined with vehicle travel behavior analysis, the CO_2 emission reduction effect can be increased by 6.5% to 13.5% in different scenarios. Considering that the increase in the proportion of non-fossil fuels in the power generation structure in the future will reduce the emission factor, the total CO_2 emissions can be reduced to 21.9% of the current CO_2 emissions at most. The benefits of reducing emission factors are not significant in the early stages of NEV promotion policies, however, in the long term, it can achieve significant CO_2 emission reduction effects. Vehicle CO_2 emissions exhibit significant spatiotemporal heterogeneity. Traffic state information, road network structure characteristics, built environment characteristics, socioeconomic attributes, and transport infrastructure characteristics are all significantly related to vehicle CO_2 emissions, with the strongest spatiotemporal correlation between road network traffic state and CO_2 emissions.

While this paper establishes the WTW CO_2 emission inventory of vehicles and explores the driving factor of gridded emission, there are still several limitations in this study. (a) Due to the sparseness of LPR devices in some districts, especially in suburban areas, some vehicle activities cannot be detected and thus were not included in our emission inventory. (b) This paper applied the average speed method in emission calculation, which ignores the acceleration and deceleration of vehicles on roads and may underestimate the emission. (c) Due to the limited number of dynamic variables, the current GTWR model focuses solely on hourly aggregate traffic volume as a time-varying variable. Other potential dynamic variables that have a significant impact on emissions might be overlooked.

In future research, we plan to combine GPS data and LPR data to capture more vehicle activities and refine the speed profile of vehicles. We hope to mine more spatiotemporal influencing factors based on multi-source data to better understand the spatiotemporal heterogeneity of CO_2 emissions. In addition, machine learning models will also be used to analyze the spatiotemporal influencing factors of CO_2 emissions. Moreover, shared mobility and intelligent connected vehicles will play significant roles in promoting sustainable development in transportation and become major trends in the future of the transportation sector [61,62]. In our subsequent research, we aim to evaluate their emission reduction effects by setting up these scenarios.

Declaration of competing interest

The authors declare that they have no conflicts of interest in this work.

Acknowledgments

This work was supported by "Pioneer" and "Leading Goose" R&D Program of Zhejiang (2023C03155), the National Natural Science Foundation of China (72361137006, 52131202, and 92046011), the Natural Science Foundation of Zhejiang Province (LR23E080002), and Alibaba-Zhejiang University Joint Research Institute of Frontier Technologies.

Supplementary materials

Supplementary material associated with this article can be found, in the online version, at doi:10.1016/j.fmre.2023.06.009.

References

[1] F. Jiang, W. He, W. Ju, et al., The status of carbon neutrality of the world's top 5 CO_2 emitters as seen by carbon satellites, Fund. Res. 2 (3) (2022) 357–366.
[2] M.A. Mateo Pla, E. Lorenzo-Sáez, J.E. Luzuriaga, et al., From traffic data to GHG emissions: a novel bottom-up methodology and its application to Valencia city, Sustain. Cities Soc. 66 (2021) 102643.
[3] Climate IPCC, Change 2022: mitigation of climate change, Contribution of Working Group III to the Sixth Assessment Report of the Intergovernmental Panel on Climate Change, Cambridge University Press, 2022.
[4] X. Li, X. Tan, R. Wu, et al., Paths for carbon peak and carbon neutrality in transport sector in China, Strat. Stud. Chin. Acad. Eng. 23 (6) (2021) 15–21 (in Chinese).
[5] Xinhua News Agency, The number of new energy vehicles in China reached 13.1 million, showing a rapid growth trend, https://www.gov.cn/xinwen/2023-01/11/content_5736281.htm, 2023 (accessed Jun. 2023)
[6] B. Cai, H. Guo, L. Cao, et al., Local strategies for China's carbon mitigation: an investigation of Chinese city-level CO_2 emissions, J. Clean. Prod. 178 (2018) 890–902.
[7] Y.H. Liu, J.L. Ma, L. Li, et al., A high temporal-spatial vehicle emission inventory based on detailed hourly traffic data in a medium-sized city of China, Environ. Pollut. 236 (2018) 324–333.
[8] F. Deng, Z. Lv, L. Qi, et al., A big data approach to improving the vehicle emission inventory in China, Nat. Commun. 11 (1) (2020) 2801.
[9] L. Jiang, Y. Xia, L. Wang, et al., Hyperfine-resolution mapping of on-road vehicle emissions with comprehensive traffic monitoring and an intelligent transportation system, Atmos. Chem. Phys. 21 (22) (2021) 16985–17002.
[10] H. Wang, K. Feng, P. Wang, et al., China's electric vehicle and climate ambitions jeopardized by surging critical material prices, Nat. Commun. 14 (1) (2023) 1246.
[11] P. Wolfram, S. Weber, K. Gillingham, et al., Pricing indirect emissions accelerates low—carbon transition of US light vehicle sector, Nat. Commun. 12 (1) (2021) 7121.
[12] B.V. Bertoncini, W.F.L. Quintanilha, L.A. Rodrigues, et al., Onboard analysis of vehicle emissions in urban ways with different functional classifications, Urban Clim. 39 (2021) 100950.
[13] N. Abdull, M. Yoneda, Y. Shimada, Traffic characteristics and pollutant emission from road transport in urban area, Air Qual. Atmos. Health 13 (2020) 731–738.
[14] R. Zhang, K. Matsushima, K. Kobayashi, Can land use planning help mitigate transport-related carbon emissions? A case of Changzhou, Land Use Policy 74 (2018) 32–40.
[15] M. Patiño-Aroca, A. Parra, R. Borge, On-road vehicle emission inventory and its spatial and temporal distribution in the city of Guayaquil, Ecuador, Sci. Total Environ. 848 (2022) 157664.

[16] S. Saija, D. Romano, A methodology for the estimation of road transport air emissions in urban areas of Italy, Atmos. Environ. 36 (34) (2002) 5377–5383.
[17] S.E. Puliafito, D. Allende, S. Pinto, et al., High resolution inventory of GHG emissions of the road transport sector in Argentina, Atmos. Environ. 101 (2015) 303–311.
[18] S. Cheng, B. Zhang, P. Peng, et al., Spatiotemporal evolution pattern detection for heavy-duty diesel truck emissions using trajectory mining: a case study of Tianjin, China, J. Clean. Prod. 244 (2020) 118654.
[19] T. Li, J. Wu, A. Dang, et al., Emission pattern mining based on taxi trajectory data in Beijing, J. Clean. Prod. 206 (2019) 688–700.
[20] J. Liu, K. Han, X.M. Chen, et al., Spatial-temporal inference of urban traffic emissions based on taxi trajectories and multi-source urban data, Transport. Res. C-Emer. 106 (2019) 145–165.
[21] X. Zhou, H. Wang, Z. Huang, et al., Identifying spatiotemporal characteristics and driving factors for road traffic CO_2 emissions, Sci. Total Environ. 834 (2022) 155270.
[22] Y. Wen, R. Wu, Z. Zhou, et al., A data-driven method of traffic emissions mapping with land use random forest models, Appl. Energ. 305 (2022) 117916.
[23] Z. Zhou, Q. Tan, H. Liu, et al., Emission characteristics and high-resolution spatial and temporal distribution of pollutants from motor vehicles in Chengdu, China, Atmos. Pollut. Res. 10 (3) (2019) 749–758.
[24] J. Wu, X. Qu, Intersection control with connected and automated vehicles: a review, J. Intell. Connect. Veh. 5 (2022) 260–269.
[25] H. Ding, W. Li, N. Xu, et al., An enhanced eco-driving strategy based on reinforcement learning for connected electric vehicles: cooperative velocity and lane-changing control, J. Intell. Connect. Veh. 5 (2022) 316–332.
[26] J. He, N. Yan, J. Zhang, et al., Battery electric buses charging schedule optimization considering time-of-use electricity price, J. Intell. Connect. Veh. 4 (2022) 138–145.
[27] J. Ji, Y. Bie, Z. Zeng, et al., Trip energy consumption estimation for electric buses, Commun. Transport. Res. 2 (2022) 100069.
[28] X.B. Qu, Y.J. Liu, Y.W. Chen, et al., Urban electric bus operation management: review and Outlook, J. Auto. Saf. Energ. 13 (3) (2022) 407–420 (in Chinese).
[29] W. Ke, S. Zhang, X. He, et al., Well-to-wheels energy consumption and emissions of electric vehicles: mid-term implications from real-world features and air pollution control progress, Appl. Energ. 188 (2017) 367–377.
[30] S. Ramachandran, S. Ulrich, Well to wheel analysis of low carbon alternatives for road traffic, Energ. Environ. Sci. 8 (11) (2015) 3313–3324.
[31] M. Gressai, B. Varga, T. Tettamanti, et al., Investigating the impacts of urban speed limit reduction through microscopic traffic simulation, Commun. Transport. Res. 1 (2021) 100018.
[32] P. Barla, L.F. Miranda-Moreno, M. Lee-Gosselin, Urban travel CO_2 emissions and land use: a case study for Quebec City, Transport. Res. D-Trans. Environ. 16 (6) (2011) 423–428.
[33] W. Yang, W. Wang, S. Ouyang, The influencing factors and spatial spillover effects of CO_2 emissions from transportation in China, Sci. Total Environ. 696 (2019) 133900.
[34] C. Barrington-Leigh, A. Millard-Ball, More connected urban roads reduce US GHG emissions, Environ. Res. Lett. 12 (4) (2017) 044008.
[35] X. Wu, T. Tao, J. Cao, et al., Examining threshold effects of built environment elements on travel-related carbon-dioxide emissions, Transport. Res. D-Trans. Environ. 75 (2019) 1–12.
[36] Z. Zhang, H.D. He, J.M. Yang, et al., Spatiotemporal evolution of NO_2 diffusion in Beijing in response to COVID-19 lockdown using complex network, Chemosphere 293 (2022) 133631.
[37] L. Pan, E. Yao, Y. Yang, Impact analysis of traffic-related air pollution based on real–time traffic and basic meteorological information, J. Environ. Manage. 183 (2016) 510–520.
[38] F. Shi, X. Liao, L. Shen, et al., Exploring the spatiotemporal impacts of urban form on CO_2 emissions: evidence and implications from 256 Chinese cities, Environ. Impact Asses. 96 (2022) 106850.
[39] W. Li, Z. Ji, F. Dong, Spatio-temporal evolution relationships between provincial CO_2 emissions and driving factors using geographically and temporally weighted regression model, Sustain. Cities Soc. 81 (2022) 103836.
[40] C. Xu, J. Zhao, L. Pan, A geographically weighted regression approach to investigate the effects of traffic conditions and road characteristics on air pollutant emissions, J. Clean. Prod. 239 (2019) 118084.
[41] J. Wu, P. Jia, T. Feng, et al., Uncovering the spatiotemporal impacts of built environment on traffic carbon emissions using multi-source big data, Land Use Policy 129 (2023) 106621.
[42] W. Yao, M. Zhang, S. Jin, et al., Understanding vehicles commuting pattern based on license plate recognition data, Transport. Res. C-Emer. 128 (2021) 103142.
[43] W. Yao, C. Chen, H. Su, et al., Analysis of key commuting routes based on spatiotemporal trip chain, J. Adv. Transport. 2022 (2022) 6044540.
[44] W. Yao, J. Yu, Y. Yang, et al., Understanding travel behavior adjustment under COVID-19, Commun. Transport. Res. 2 (2022) 100068.
[45] X. Chang, J. Wu, Z. He, et al., Understanding user's travel behavior and city region functions from station-free shared bike usage data, Transport. Res. F-Traf. 72 (2020) 81–95.
[46] R. Li, Z. Liu, R. Zhang, Studying the benefits of carpooling in an urban area using automatic vehicle identification data, Transport. Res. C-Emer. 93 (2018) 367–380.
[47] Z. Yu, W. Li, Y. Liu, et al., Quantification and management of urban traffic emissions based on individual vehicle data, J. Clean. Prod. 328 (2021) 129386.
[48] H. Yu, S. Yang, Z. Wu, et al., Vehicle trajectory reconstruction from automatic license plate reader data, Int. J. Distrib. Sens. Netw. 14 (2) (2018) 1550147718755637.
[49] X. Jing, S. Ren, X. Wang, T. Li, et al., Basic ideas and development trend of heavy–duty vehicle emission regulations in next stage, J. Auto. Saf. Energ. 14 (2023) 133–156.
[50] Z. Chen, Review on the research and development trends and prospects for argon closed cycle hydrogen engines, J. Auto. Saf. Energ. 14 (2023) 1–16.
[51] X. Ma, Y. Ji, Y. Yuan, et al., A comparison in travel patterns and determinants of user demand between docked and dockless bike-sharing systems using multi-sourced data, Transport. Res. A-Pol. Pract. 139 (2020) 148–173.
[52] X. Shen, Y. Zhou, S. Jin, et al., Spatiotemporal influence of land use and household properties on automobile travel demand, Transport. Res. D-Trans. Environ. 84 (2020) 102359.
[53] B. Wu, R. Li, B. Huang, A geographically and temporally weighted autoregressive model with application to housing prices, Int. J. Geogr. Inf. Sci. 28 (5) (2014) 1186–1204.
[54] C.M. Hurvich, J.S. Simonoff, C.L. Tsai, Smoothing parameter selection in nonparametric regression using an improved akaike information criterion, J. R. Stat. Soc. 60 (1998) 271–293.
[55] B. Huang, B. Wu, M. Barry, Geographically and temporally weighted regression for modeling spatio-temporal variation in house prices, Int. J. Geogr. Inf. Sci 24 (3) (2010) 383–401.
[56] F. An, L.P. Kang, L.Z. Qin, et al., A study on China's timetable for phasing-out traditional ice-vehicles, Int. Petrol. Econ. 27 (5) (2019) 1–8 in Chinese.
[57] R. Opoku, B. Ahunu, G.K.K. Ayetor, et al., Unlocking the potential of solar electric vehicles for post-COVID recovery and growth in the transport sector in Ghana, Sci. Afr. 20 (2023) e01583.
[58] C. Redl, F. Hein, M. Buck, et al., The European Power Sector in 2020: Up-to-Date Analysis on the Electricity Transition, Agora Energiewende, 2021.
[59] J. He, Z. Li, X. Zhang X, et al., Towards carbon neutrality: a study on China's long-term low-carbon transition pathways and strategies, Environ. Sci. Ecotech. 9 (2022) 100134.
[60] H. Duan, S. Zhou, K. Jiang, et al., Assessing China's efforts to pursue the 1.5 C warming limit, Science 372 (6540) (2021) 378–385.
[61] M. Attard, Active travel and sustainable transport, Commun. Transport. Res. 2 (2022) 100059.
[62] A. Ansariyar, M. Tahmasebi, Investigating the effects of gradual deployment of market penetration rates (MPR) of connected vehicles on delay time and fuel consumption, J. Intell. Connect. Veh. 5 (3) (2022) 188–198.

Zuoming Zhang is currently a M.S. candidate in the Polytechnic Institute & Institute of Intelligent Transportation Systems, Zhejiang University. He focuses on spatiotemporal big data mining and urban transportation emission analysis.

Hongyang Su is currently pursuing the M.S. degree in the Polytechnic Institute & Institute of Intelligent Transportation Systems, Zhejiang University. He received the bachelor's degree in traffic engineering from Southeast University in 2021. His research interests include traffic big data, carbon neutrality in the transport sector, and travel behavior analysis.

Wenbin Yao received the B.S. degree and Ph.D. degree from Zhejiang University. He is currently a lecturer with the School of Civil Engineering and Architecture, Zhejiang Sci-Tech University. His research interests include traffic demand management, and data-driven transportation system modeling and analysis.

Sheng Jin (BRID: 08367.00.29768) received the Ph.D. degree in Transportation Engineering from Jilin University, Changchun, China, in 2010. Now, he is a professor with the College of Civil Engineering and Architecture, Zhejiang University, Hangzhou, China. He has published more than 80 articles in related journals such as *Transportation Research part A/B/C/D, Accident Analysis & Prevention, IEEE T ITS, and IEEE ITSM*. His research is focused on traffic flow theory, intelligent transportation systems, traffic signal control, and traffic big data.